

Free-Space Fundamental Solution of a 2D Steady Slow Viscous MHD Flow

A. Sellier¹, S. H. Aydin² and M. Tezer-Sezgin³

Abstract: The fundamental free-space 2D steady creeping MHD flow produced by a concentrated point force of strength \mathbf{g} located at a so-called source point \mathbf{x}_0 in an unbounded conducting Newtonian liquid with uniform viscosity μ and conductivity $\sigma > 0$ subject to a prescribed uniform ambient magnetic field $\mathbf{B} = B\mathbf{e}_1$ is analytically obtained. More precisely, not only the produced flow pressure p and velocity \mathbf{u} but also the resulting stress tensor field $\boldsymbol{\sigma}$ are expressed at any observation point $\mathbf{x} \neq \mathbf{x}_0$ in terms of usual modified Bessel functions, the vectors $\mathbf{g}, \mathbf{x} - \mathbf{x}_0$ and the so-called Hartmann layer thickness $d = (\sqrt{\mu/\sigma})/B$ (see Hartmann (1937)). The resulting basic flows obtained for \mathbf{g} either parallel with or normal to the magnetic field \mathbf{B} are examined and found to exhibit quite different properties.

Keywords: MagnetoHydroDynamics, Two-dimensional flow, Stokes flow, Fundamental solution, Green tensor, Hartmann layer thickness, modified Bessel functions.

1 Introduction

A conducting liquid with uniform conductivity $\sigma > 0$ flows when subject to ambient magnetic and/or electric field(s). Such a flow, with pressure p and velocity \mathbf{u} , is actually driven by the (non-uniform) Lorentz body-force $\mathbf{f} = \mathbf{j} \wedge \mathbf{B}$ with \mathbf{j} the current density given from Ohm's law by $\mathbf{j} = \sigma(\mathbf{E} + \mathbf{u} \wedge \mathbf{B})$ where \mathbf{B} and \mathbf{E} designate the magnetic and electric fields prevailing in the liquid. The determination of the quantities $p, \mathbf{u}, \mathbf{B}$ and \mathbf{E} falls in the field of MagnetoHydrodynamics (see, for instance, Moreau (1990)) and is in general tedious since such quantities obey *coupled* incompressible non-linear Navier-Stokes equations with body force \mathbf{f} for the so-called MHD flow (\mathbf{u}, p) and Maxwell equations for (\mathbf{E}, \mathbf{B}) . Even more involved is the case when solid particles are suspended in the conducting liquid. As

¹ LadHyX, École Polytechnique, 91128 Palaiseau cedex. France.

² Department of Mathematics, Karadeniz Technical University, 61080, Trabzon, TURKEY.

³ Department of Mathematics, Middle East Technical University, 06531, Ankara, TURKEY.

discussed in Gotoh (1960), for some steady MHD flows exhibiting specific symmetries the previous equations fortunately decouple in the sense one is then able to first get the fields \mathbf{B} and \mathbf{E} prior to the determination of the MHD flow (\mathbf{u}, p) . It might even happen that in the entire liquid domain $(\mathbf{B}, \mathbf{E}) = (\mathbf{B}, \mathbf{0})$ with \mathbf{B} uniform! This is the case for the following cases:

- (i) A solid sphere translating in a quiescent liquid parallel with a prescribed uniform external magnetic field \mathbf{B} in absence of far-field electric field (see Chester (1957)).
- (ii) The plane steady two-dimensional MHD flow produced by the rigid-body motion (translation parallel with and/or rotation normal to the plane) of a solid particle in a conducting quiescent fluid solely subject (no far-field electric field) to a uniform magnetic field \mathbf{B} lying in the flow plane. Such a 2D case is illustrated in Fig. 1.

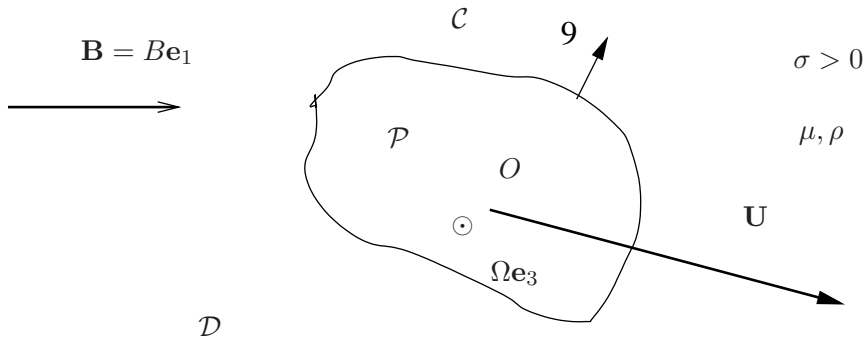


Figure 1: A solid plane particle P , with (closed) boundary C , immersed in the ambient uniform magnetic field $\mathbf{B} = B\mathbf{e}_1$ and migrating with translational velocity \mathbf{U} and/or angular velocity $\Omega\mathbf{e}_3$.

If the particle has length scale a and its rigid-body motion velocity has typical magnitude $U > 0$ the MHD flow Reynolds number $Re = \rho U a / \mu$ may be of quite different magnitude depending upon the applications. Whenever Re is moderate or large getting the MHD flow about the moving solid body remains a very-involved task even in above Cases (i)-(ii), for which there is no electric field and a prescribed uniform magnetic field, because one has still to cope with the non-linear Navier-Stokes equations. Fortunately, for some applications involving small solid particles one has $Re \ll 1$ and, neglecting inertial effects, the MHD flow then obeys the more tractable (linear) Stokes equations. Within this framework Yosinobu and Kabutani (1959) solved Case (ii) for a translating disk by expanding the flow stream function

as an infinite series of terms and truncating the series for the computations. The Reynolds number compares in the Navier-Stokes equations the inertial term with the viscous term. As previously outlined, the MHD flow is driven by the Lorentz body-force. Comparing in the Navier-Stokes equations this force with the viscous term gives the Hartmann number M . This number is obtained by introducing the so-called Hartmann layer thickness d [Hartmann (1937)]. For a magnetic field with typical magnitude $B > 0$ the Hartmann length d and number M read

$$d = (\sqrt{\mu/\sigma})/B, \quad M = a/d. \quad (1)$$

The low-Reynolds-number MHD flow about the solid particle in Cases (i)-(ii) has been then found to deeply depend upon the value of M [Chester (1957); Yosinobu and Kabutani (1959)].

For applications one might of course encounter solid particles which are not disks. Unfortunately, it is not possible to extend the method employed in Yosinobu and Kabutani (1959) for the translating disk to deal for a solid body of arbitrary (but smooth) shape. Therefore, another technique is needed to deal with the 2D problem (ii) of a solid and arbitrary-shaped body experiencing a given rigid-body motion (translation and/or rotation) and subject to a given uniform magnetic field \mathbf{B} . One can think about extending the boundary approach available for a 2D Stokes in absence of magnetic field [Pozrikidis (1992)]. To do so the key step consists in obtaining the so-called fundamental flow associated with the considered problem, i. e. the free-space 2D steady creeping MHD flow produced by a concentrated point force of strength \mathbf{g} located at a source point \mathbf{x}_0 in the plane domain. Such a challenging issue is addressed in the present work.

The paper is organized as follows. The governing 2D problem and the velocity, pressure and stress tensor associated with the required fundamental MHD Stokes flow are analytically obtained in §2. Two different basic flows are then distinguished and studied (paying attention to each flow pattern) in §3. Finally, a few remarks in §4 close the paper.

2 Fundamental flow problem and analytical solution

This section gives the governing 2D MHD problem for the fundamental flow and derives the associated analytical solution.

2.1 Governing flow problem and notations

We look at the so-called free-space fundamental 2D MHD plane steady Stokes flow with pressure field p and velocity field \mathbf{u} produced in a Newtonian liquid, where

prevails the uniform magnetic field \mathbf{B} , by a concentrated point force of strength \mathbf{g} placed at the arbitrary source point \mathbf{x}_0 . We adopt Cartesian coordinates (O, x_1, x_2) and take $\mathbf{B} = B\mathbf{e}_1$ with $B > 0$. Denoting by $\mu > 0$ and $\sigma > 0$ the uniform liquid viscosity and conductivity, the flow (\mathbf{u}, p) then obeys the following steady Stokes equations and far-field behaviour

$$\nabla \cdot \mathbf{u} = 0 \text{ for } \mathbf{x} \neq \mathbf{x}_0, \quad (2)$$

$$\mu \nabla^2 \mathbf{u} + \sigma B^2 (\mathbf{u} \wedge \mathbf{e}_1) \wedge \mathbf{e}_1 - \nabla p = -\delta(\mathbf{x} - \mathbf{x}_0) \mathbf{g} \text{ for } \mathbf{x} \neq \mathbf{x}_0, \quad (3)$$

$$(\mathbf{u}, p) \rightarrow (\mathbf{0}, 0) \text{ as } |\mathbf{x} - \mathbf{x}_0| \rightarrow \infty \quad (4)$$

where δ is the two-dimensional delta pseudo-function.

Inspecting (2)-(4) immediately shows that (\mathbf{u}, p) and its stress tensor σ lineary depend upon the force \mathbf{g} . As in Pozrikidis (1992), we thus introduce a Green vector \mathbf{P} and a so-called second-rank Green velocity tensor \mathbf{G} such that

$$\mathbf{u}(\mathbf{x}) = \frac{1}{4\pi\mu} \mathbf{G}(\mathbf{x}, \mathbf{x}_0) \cdot \mathbf{g}, \quad p(\mathbf{x}) = \frac{1}{4\pi} \mathbf{P}(\mathbf{x}, \mathbf{x}_0) \cdot \mathbf{g}. \quad (5)$$

The aim of the present work is to determine those Green vector $\mathbf{P}(\mathbf{x}, \mathbf{x}_0)$ and tensor $\mathbf{G}(\mathbf{x}, \mathbf{x}_0)$ at $\mathbf{x} \neq \mathbf{x}_0$ whatever the value (recall the definitions (1)) of the Hartmann layer thickness $d = (\sqrt{\mu/\sigma})/B$. Knowing such quantities will also permit us to subsequently obtain the associated stress tensor σ .

2.2 Velocity second-rank Green tensor

Henceforth, we adopt the tensor summation convention. For instance we have $\mathbf{x} = x_i \mathbf{e}_i$ and $\mathbf{u} = u_i \mathbf{e}_i$. Under such notations the force strength \mathbf{g} is $\mathbf{g} = g_i \mathbf{e}_i$. Similarly, the tensor $\mathbf{G}(\mathbf{x}, \mathbf{x}_0)$ admits Cartesian components $G_{ij}(\mathbf{x}, \mathbf{x}_0)$ with $\mathbf{G}(\mathbf{x}, \mathbf{x}_0) = G_{ij}(\mathbf{x}, \mathbf{x}_0) \mathbf{e}_i \otimes \mathbf{e}_j$.

Clearly, (2)-(4) show that $\mathbf{G}(\mathbf{x}, \mathbf{x}_0) = \mathbf{G}(\mathbf{x} - \mathbf{x}_0)$ and $\mathbf{P}(\mathbf{x}, \mathbf{x}_0) = \mathbf{P}(\mathbf{x} - \mathbf{x}_0)$. Accordingly, we restrict our attention to the case of a concentrated force located at the origin O (case $\mathbf{x}_0 = \mathbf{0}$).

As outlined in the introduction, determining the Green tensor \mathbf{G} is a key task for a future boundary approach of the 2D MHD slow viscous flow about a solid particle experiencing a given rigid-body motion. As always when dealing with either two-dimensional or three-dimensional Stokes fundamental flows, one can think about using a direct approach (as, for instance, in Sellier (2008)) or a Fourier transform (as in Jones (2004) or Sellier and Pasol (2006) for the fundamental flow between two plane and parallel walls and also as recently achieved in Sellier and Ghalia

(2011) for the fundamental flow above a plane slip wall with a general anisotropic slip condition).

In this work we adopt a direct approach and obtain the required Green tensor \mathbf{G} by micmicking the nice treatment worked out in Priede (2013) for a similar three-dimensional problem. In order to get ride of the pressure p we first apply the operator $\nabla \wedge (\nabla \wedge)$ to each side of equation (3). Taking into account of the continuity equation (2) we arrive at

$$\mu \nabla^2 (\nabla^2 \mathbf{u}) - \sigma B^2 \frac{\partial^2 \mathbf{u}}{\partial x_1^2} = \nabla \wedge (\nabla \wedge [\delta \mathbf{g}]) \quad (6)$$

with $\mathbf{u} = \mathbf{u}(\mathbf{x})$, $\delta = \delta(\mathbf{x})$ and $\mathbf{x} = x_1 \mathbf{e}_1 + x_2 \mathbf{e}_2$. Denoting by Δ the usual two-dimensional Laplacien operator, the solution for the velocity \mathbf{u} then reads

$$\mathbf{u} = \frac{1}{\mu} \nabla \wedge (\nabla \wedge [H \mathbf{g}]), \quad (7)$$

$$\Delta(\Delta H) - \frac{\sigma B^2}{\mu} \frac{\partial^2 H}{\partial x_1^2} = \delta \quad (8)$$

where the occurring function H has to be determined. Observe that knowing H will immediately provide the velocity $\mathbf{u} = u_1 \mathbf{e}_1 + u_2 \mathbf{e}_2$ from (7) by appealing to the relations (recall that $\mathbf{g} = g_i \mathbf{e}_i$)

$$\mu u_1 = \left[\frac{\partial^2 H}{\partial x_1^2} - \Delta H \right] g_1 + \left[\frac{\partial^2 H}{\partial x_2 \partial x_1} \right] g_2, \quad (9)$$

$$\mu u_2 = \left[\frac{\partial^2 H}{\partial x_2 \partial x_1} \right] g_1 + \left[\frac{\partial^2 H}{\partial x_2^2} - \Delta H \right] g_2. \quad (10)$$

By virtue of (9)-(10), it turns out that it is sufficient to determine the functions ΔH and $\partial H / \partial x_1$ (the obtention of H is therefore not needed).

Here, the function H is gained by solving the problem (8) with a proper far-field behaviour. For convenience, we recognize on the left-hand side of (8) the quantity $1/d^2$ with $d = (\sqrt{\mu/\sigma})/B$ the Hartmann layer thickness (see also (1)). We also introduce two auxiliary functions H_- and H_+ as follows

$$\left[\Delta + \frac{1}{d} \frac{\partial}{\partial x_1} \right] H_- = \left[\Delta - \frac{1}{d} \frac{\partial}{\partial x_1} \right] H_+ = -\delta, \quad (11)$$

$$\Delta H = -\frac{H_+ + H_-}{2}, \quad \frac{\partial H}{\partial x_1} = -\frac{d}{2}(H_+ - H_-). \quad (12)$$

Because both u_1 and u_2 are required to vanish far from the source point O (recall the far-field behaviour (4)) we must retain functions H_- and H_+ going to zero as $r = |\mathbf{x}|$ becomes large. Designating by K_0 the usual modified Bessel function of order zero (which indeed vanishes at infinity; see Abramowitz and Stegun (1965)) and also using Pozrikidis (2002), the required solutions are found to be

$$H_{\pm} = \frac{1}{2\pi} e^{\pm x_1/(2d)} K_0\left(\frac{r}{2d}\right). \tag{13}$$

Therefore, one gets

$$\Delta H = -\frac{1}{2\pi} \cosh\left(\frac{x_1}{2d}\right) K_0\left(\frac{r}{2d}\right), \tag{14}$$

$$\frac{\partial H}{\partial x_1} = -\frac{d}{2\pi} \sinh\left(\frac{x_1}{2d}\right) K_0\left(\frac{r}{2d}\right). \tag{15}$$

Invoking (9)-(10) and the definitions (5) easily provides the required Cartesian components $G_{ij}(\mathbf{x}, \mathbf{x}_0)$ of the second-rank Green velocity tensor. Because $K'_0 = -K_1$, with K_1 the usual modified Bessel function of order one, the obtained results read

$$G_{11}(\mathbf{x}, \mathbf{x}_0) = \cosh\left(\frac{\hat{x}_1}{2d}\right) K_0\left(\frac{\hat{r}}{2d}\right) + \sinh\left(\frac{\hat{x}_1}{2d}\right) K_1\left(\frac{\hat{r}}{2d}\right) \frac{\hat{x}_1}{\hat{r}}, \tag{16}$$

$$G_{12}(\mathbf{x}, \mathbf{x}_0) = \sinh\left(\frac{\hat{x}_1}{2d}\right) K_1\left(\frac{\hat{r}}{2d}\right) \frac{\hat{x}_2}{\hat{r}}, \tag{17}$$

$$G_{21}(\mathbf{x}, \mathbf{x}_0) = G_{12}(\mathbf{x}, \mathbf{x}_0), \tag{18}$$

$$G_{22}(\mathbf{x}, \mathbf{x}_0) = \cosh\left(\frac{\hat{x}_1}{2d}\right) K_0\left(\frac{\hat{r}}{2d}\right) - \sinh\left(\frac{\hat{x}_1}{2d}\right) K_1\left(\frac{\hat{r}}{2d}\right) \frac{\hat{x}_1}{\hat{r}} \tag{19}$$

with the notations $\hat{\mathbf{x}} = \mathbf{x} - \mathbf{x}_0$, $\hat{x}_i = \hat{\mathbf{x}} \cdot \mathbf{e}_i$ and $\hat{r} = |\hat{\mathbf{x}}|$. The derived Cartesian components of the Green velocity tensor are thus found to obey the following properties: $G_{ij}(\mathbf{x}, \mathbf{x}_0) = G_{ji}(\mathbf{x}_0, \mathbf{x}) = G_{ij}(\mathbf{x}_0, \mathbf{x})$.

2.3 Pressure Green vector

We now look at the pressure Green vector $\mathbf{P}(\mathbf{x}, \mathbf{x}_0)$ introduced by (5). To do so we need to determine the pressure p for the fundamental flow. Selecting again $\mathbf{x}_0 = \mathbf{0}$, we appeal to the equation (3) which now reads $\nabla p = \mu \nabla^2 \mathbf{u} + \sigma B^2 (\mathbf{u} \wedge \mathbf{e}_1) \wedge \mathbf{e}_1 + \delta(\mathbf{x}) \mathbf{g}$ with \mathbf{u} previously given by (7) and (9)-(10). Taking the divergence of this equation and using the property $\nabla \cdot \mathbf{u} = 0$ gives $\Delta p = \nabla \cdot (\delta \mathbf{g}) + \sigma B^2 \nabla \cdot [(\mathbf{u} \cdot \mathbf{e}_1) \mathbf{e}_1]$. Applying now on each side the Laplacien operator easily gives for the pressure p the equation

$$\Delta(\Delta p) - \frac{\sigma B^2}{\mu} \frac{\partial^2 p}{\partial x_1^2} = \Delta[\nabla \cdot (\delta \mathbf{g})] - \frac{\sigma B^2 [\mathbf{g} \cdot \mathbf{e}_1]}{\mu} \frac{\partial \delta}{\partial x_1}. \tag{20}$$

Recalling that H obeys (8) and using the definition (1) of the Hartmann layer thickness d then provides the pressure p . One ends up with the solution

$$p = \Delta[\nabla \cdot (H\mathbf{g})] - \left(\frac{\mathbf{g} \cdot \mathbf{e}_1}{d^2}\right) \frac{\partial H}{\partial x_1} = \left[\frac{\partial \Delta H}{\partial x_1} - \frac{1}{d^2} \frac{\partial H}{\partial x_1}\right] g_1 + \left[\frac{\partial}{\partial x_2} (\Delta H)\right] g_2. \tag{21}$$

Accordingly, one arrives at the following components $P_i = \mathbf{P} \cdot \mathbf{e}_i$ for the pressure Green tensor

$$P_1(\mathbf{x}, \mathbf{x}_0) = \frac{1}{d} \left[\sinh\left(\frac{\hat{x}_1}{2d}\right) K_0\left(\frac{\hat{r}}{2d}\right) + \cosh\left(\frac{\hat{x}_1}{2d}\right) K_1\left(\frac{\hat{r}}{2d}\right) \frac{\hat{x}_1}{\hat{r}} \right], \tag{22}$$

$$P_2(\mathbf{x}, \mathbf{x}_0) = \frac{1}{d} \cosh\left(\frac{\hat{x}_1}{2d}\right) K_1\left(\frac{\hat{r}}{2d}\right) \frac{\hat{x}_2}{\hat{r}}. \tag{23}$$

2.4 Associated third-rank Green stress tensor

In this subsection we gain the stress tensor σ for the fundamental flow (\mathbf{u}, p) from the previous results established for the fields \mathbf{u} and p . Still using our tensor summation notation, the flow (\mathbf{u}, p) has stress tensor $\sigma(\mathbf{x}) = \sigma_{ij}(\mathbf{x}, \mathbf{x}_0) \mathbf{e}_i \otimes \mathbf{e}_j$. By linearity, one can introduce a so-called third-rank stress tensor \mathbf{T} with cartesian components $T_{ijk}(\mathbf{x}, \mathbf{x}_0)$ such that (see also Pozrikidis (1992))

$$\sigma_{ik}(\mathbf{x}, \mathbf{x}_0) = \frac{1}{4\pi} T_{ijk}(\mathbf{x}, \mathbf{x}_0) g_j. \tag{24}$$

One should here carefully note by that our definition (24) does not at that stage read $\sigma = \mathbf{T} \cdot \mathbf{g}$! Using the definitions (5) and (24) immediately shows that

$$T_{ijk}(\mathbf{x}, \mathbf{x}_0) = -\delta_{ik} P_j(\mathbf{x}, \mathbf{x}_0) + \frac{\partial G_{ij}}{\partial x_k}(\mathbf{x}, \mathbf{x}_0) + \frac{\partial G_{kj}}{\partial x_i}(\mathbf{x}, \mathbf{x}_0) \tag{25}$$

where the symbol δ_{ik} designates the Kronecker delta. Hence, $T_{ijk} = T_{kji}$ and the task therefore reduces to the determination of only six Cartesian components of the stress tensor: the components $T_{111}, T_{121}, T_{212}, T_{222}$ and the components $T_{112} = T_{211}$ and $T_{122} = T_{221}$. After elementary manipulations one gets, using the results (16)-(19) and (22)-(23),

$$T_{111}(\mathbf{x}, \mathbf{x}_0) = 2 \sinh\left(\frac{\hat{x}_1}{2d}\right) K_1\left(\frac{\hat{r}}{2d}\right) \left(\frac{1}{\hat{r}} - \frac{\hat{x}_1^2}{\hat{r}^3}\right) + \frac{1}{d} \left[\sinh\left(\frac{\hat{x}_1}{2d}\right) K_1'\left(\frac{\hat{r}}{2d}\right) \frac{\hat{x}_1}{\hat{r}} - \cosh\left(\frac{\hat{x}_1}{2d}\right) K_1\left(\frac{\hat{r}}{2d}\right) \right] \frac{\hat{x}_1}{\hat{r}}, \tag{26}$$

$$T_{222}(\mathbf{x}, \mathbf{x}_0) = -\frac{2}{d} \cosh\left(\frac{\hat{x}_1}{2d}\right) K_1\left(\frac{\hat{r}}{2d}\right) \frac{\hat{x}_2}{\hat{r}} + \sinh\left(\frac{\hat{x}_1}{2d}\right) \left[\frac{2}{\hat{r}} K_1\left(\frac{\hat{r}}{2d}\right) - \frac{1}{d} K_1'\left(\frac{\hat{r}}{2d}\right) \right] \frac{\hat{x}_1 \hat{x}_2}{\hat{r}^2}, \tag{27}$$

$$T_{121}(\mathbf{x}, \mathbf{x}_0) = 2 \sinh\left(\frac{\hat{x}_1}{2d}\right) \left[\frac{1}{2d} K_1'\left(\frac{\hat{r}}{2d}\right) - \frac{1}{\hat{r}} K_1\left(\frac{\hat{r}}{2d}\right) \right] \times \left(\frac{\hat{x}_1 \hat{x}_2}{\hat{r}^2}\right) \tag{28}$$

and also

$$\begin{aligned} T_{212}(\mathbf{x}, \mathbf{x}_0) &= \frac{1}{d} \sinh\left(\frac{\hat{x}_1}{2d}\right) \left[K_1'\left(\frac{\hat{r}}{2d}\right) \frac{\hat{x}_2^2}{\hat{r}^2} - K_0\left(\frac{\hat{r}}{2d}\right) \right] \\ &\quad - \frac{1}{d} \cosh\left(\frac{\hat{x}_1}{2d}\right) K_1\left(\frac{\hat{r}}{2d}\right) \frac{\hat{x}_1}{\hat{r}} \\ &\quad + 2 \sinh\left(\frac{\hat{x}_1}{2d}\right) K_1\left(\frac{\hat{r}}{2d}\right) \left(\frac{1}{\hat{r}} - \frac{\hat{x}_2^2}{\hat{r}^3}\right), \end{aligned} \tag{29}$$

$$\begin{aligned} T_{112}(\mathbf{x}, \mathbf{x}_0) &= T_{211}(\mathbf{x}, \mathbf{x}_0) \\ &= \sinh\left(\frac{\hat{x}_1}{2d}\right) \left[\frac{1}{d} K_1'\left(\frac{\hat{r}}{2d}\right) - \frac{2}{\hat{r}} K_1\left(\frac{\hat{r}}{2d}\right) \right] \frac{\hat{x}_1 \hat{x}_2}{\hat{r}^2}, \end{aligned} \tag{30}$$

$$\begin{aligned} T_{122}(\mathbf{x}, \mathbf{x}_0) &= T_{221}(\mathbf{x}, \mathbf{x}_0) \\ &= \frac{1}{2d} \sinh\left(\frac{\hat{x}_1}{2d}\right) K_0\left(\frac{\hat{r}}{2d}\right) - \frac{1}{d} \cosh\left(\frac{\hat{x}_1}{2d}\right) K_1\left(\frac{\hat{r}}{2d}\right) \frac{\hat{x}_1}{\hat{r}} \\ &\quad + \sinh\left(\frac{\hat{x}_1}{2d}\right) \left[\frac{1}{\hat{r}} K_1\left(\frac{\hat{r}}{2d}\right) - \frac{1}{2d} K_1'\left(\frac{\hat{r}}{2d}\right) \right] \left[\frac{\hat{x}_1^2 - \hat{x}_2^2}{\hat{r}^2} \right] \end{aligned} \tag{31}$$

where K_1' designates the derivative of the function K_1 and of course $\hat{\mathbf{x}} = \mathbf{x} - \mathbf{x}_0$, $\hat{x}_i = \hat{\mathbf{x}} \cdot \mathbf{e}_i$ and $\hat{r} = |\hat{\mathbf{x}}|$. Observe that $T_{ijk}(\mathbf{x}, \mathbf{x}_0) = -T_{ijk}(\mathbf{x}_0, \mathbf{x})$.

3 Properties of the fundamental flows produced by a point force parallel or normal to the magnetic field

By linearity, two different fundamental flows actually occur: the first one for a unit force $\mathbf{g} = \mathbf{e}_1$ parallel with \mathbf{B} and the second one for a unit force $\mathbf{g} = \mathbf{e}_2$ normal to \mathbf{B} . As seen in this section, such basic fundamental flows actually exhibit quite different properties.

3.1 Distinguished key fundamental flows and associated near-field and far-field behaviours

Let us introduce two fundamentals flows $\mathbf{u}^{(p)}$ and $\mathbf{u}^{(n)}$ obtained by putting a source at the point \mathbf{x}_0 with unit strength $\mathbf{g} = \mathbf{e}_1$ and $\mathbf{g} = \mathbf{e}_2$, respectively. At each point $\mathbf{x} \neq \mathbf{x}_0$ one thus has

$$\bar{\mathbf{u}}^{(p)} := 4\pi\mu\mathbf{u}^{(p)}(\mathbf{x}) = G_{11}(\mathbf{x}, \mathbf{x}_0)\mathbf{e}_1 + G_{21}(\mathbf{x}, \mathbf{x}_0)\mathbf{e}_2, \tag{32}$$

$$\bar{\mathbf{u}}^{(n)} := 4\pi\mu\mathbf{u}^{(n)}(\mathbf{x}) = G_{12}(\mathbf{x}, \mathbf{x}_0)\mathbf{e}_1 + G_{22}(\mathbf{x}, \mathbf{x}_0)\mathbf{e}_2 \quad (33)$$

and for the associated pressures $p^{(p)}$ and $p^{(n)}$

$$\bar{p}^{(p)} := 4\pi d p^{(p)}(\mathbf{x}) = dP_1(\mathbf{x}, \mathbf{x}_0), \quad (34)$$

$$\bar{p}^{(n)} := 4\pi d p^{(n)}(\mathbf{x}) = dP_2(\mathbf{x}, \mathbf{x}_0). \quad (35)$$

As introduced in §2.2, we note $\hat{\mathbf{x}} = \mathbf{x} - \mathbf{x}_0 = \hat{x}_i\mathbf{e}_i$ and $\hat{r} = |\hat{x}|$. The near-field ($\hat{r} \rightarrow 0$) and far-field ($\hat{r} \rightarrow \infty$) behaviours of the previous flows are thus obtained by using the following asymptotic behaviours (see Abramowitz and Stegun (1965))

$$K_0(\alpha) \sim -\log \alpha \text{ and } K_1(\alpha) \sim 1/\alpha \text{ as } \alpha \rightarrow 0^+, \quad (36)$$

$$K_0(\alpha) \sim K_1(\alpha) \sim \sqrt{\frac{\pi}{2\alpha}} e^{-\alpha} \text{ as } \alpha \rightarrow \infty. \quad (37)$$

Accordingly, one gets for the near-field

$$G_{11} \sim G_{22} \sim -\log \hat{r}, \quad G_{12} = G_{21} \sim \frac{\hat{x}_1 \hat{x}_2}{\hat{r}^2} \text{ as } \hat{r} \rightarrow 0 \quad (38)$$

and for the far-field ($\hat{r} \rightarrow \infty$)

$$G_{12} = G_{21} \sim \frac{\hat{x}_1}{2|\hat{x}_1|} \sqrt{\frac{\pi d}{\hat{r}}} e^{(|\hat{x}_1| - \hat{r})/(2d)} \frac{\hat{x}_2}{\hat{r}} \quad (\hat{x}_1 \neq 0), \quad (39)$$

$$G_{11} \sim \frac{1}{2} \sqrt{\frac{\pi d}{\hat{r}}} e^{(|\hat{x}_1| - \hat{r})/(2d)} \left[1 + \frac{|\hat{x}_1|}{\hat{r}}\right], \quad (40)$$

$$G_{22} \sim \frac{1}{2} \sqrt{\frac{\pi d}{\hat{r}}} e^{(|\hat{x}_1| - \hat{r})/(2d)} \left[1 - \frac{|\hat{x}_1|}{\hat{r}}\right]. \quad (41)$$

Inspecting (39)-(41) shows an exponential decay of the components G_{ij} when $\hat{x}_2 \neq 0$. In contrast, for $\hat{x}_2 = 0$ and $|\hat{x}_1| = \hat{r}$ large it appears that $G_{12} = G_{21} = G_{22} \sim 0$ while $G_{11} \sim \sqrt{\pi d/|\hat{x}_1|}$ and thus decays much more slowly. As a consequence, the flow $\bar{\mathbf{u}}^{(n)}$ decays faster than the flow $\bar{\mathbf{u}}^{(p)}$ which has a component parallel with the magnetic field slowly decaying close to the $\hat{x}_2 = 0$ axis.

3.2 Flow patterns

Both velocity patterns $\bar{\mathbf{u}}^{(p)}$ and $\bar{\mathbf{u}}^{(n)}$ are now plotted versus the normalized coordinates $x'_i = \hat{x}_i/d$. For comparison purposes we first plot in Fig. 2-4 the velocity components of those flows.

These flows admit the same velocity in the direction normal to the associated unit force (because $G_{12} = G_{21}$). In contrast, the velocity component along the direction

of the unit force is very different from one flow to the other one (compare Fig. 2 and Fig. 4). Moreover, one clearly sees in Fig. 2 the slow decay of the velocity component $\bar{\mathbf{u}}^{(p)} \cdot \mathbf{e}_1$ near the $x'_2 = 0$ axis. Actually, for the flow $\bar{\mathbf{u}}^{(p)}$ the velocity magnitude is given by its component parallel with the uniform magnetic field $\mathbf{B} = B\mathbf{e}_1$ which is larger than the component normal to \mathbf{B} .

Finally, we also draw in Fig. 5-6 each flow streamlines pattern. Again, quite different streamlines are obtained for the two different flows. As expected (see Fig. 5), the streamlines for the flow $\bar{\mathbf{u}}^{(p)}$ are nearly parallel with the magnetic field in a large domain near the $x'_2 = 0$ axis or far away from the source point.

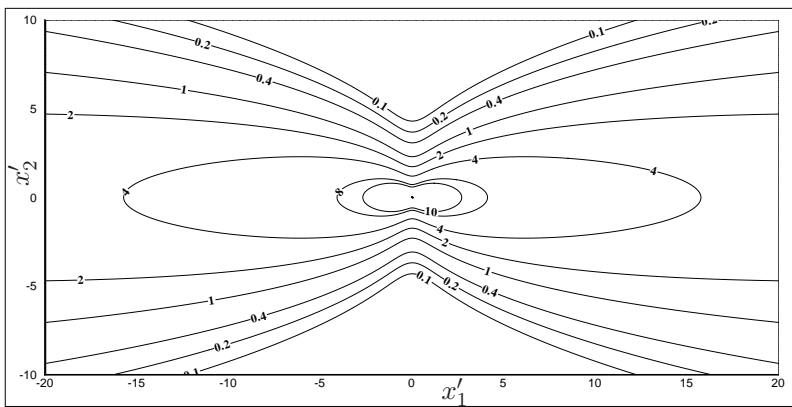


Figure 2: Isolevel contours for the velocity component $\bar{\mathbf{u}}^{(p)} \cdot \mathbf{e}_1 = G_{11}(\mathbf{x}, \mathbf{x}_0)$ in the plane (x'_1, x'_2) .

4 Conclusions

The 2D MHD Stokes flow produced by a point force has been analytically obtained. Not only the velocity field but also the pressure and the stress tensor have been given in closed form. The solution is found to deeply depend upon the Hartmann layer thickness and to exponentially decay far from the source except for the velocity component parallel with the magnetic field \mathbf{B} when the force is not normal to \mathbf{B} . Two basic flows obtained when the force is normal or parallel with \mathbf{B} have been introduced and found to exhibit quite different far-field behaviours. The material presented in this paper is a first key step in developing a boundary approach to determine the 2D MHD Stokes flow about a solid particle of arbitrary shape and

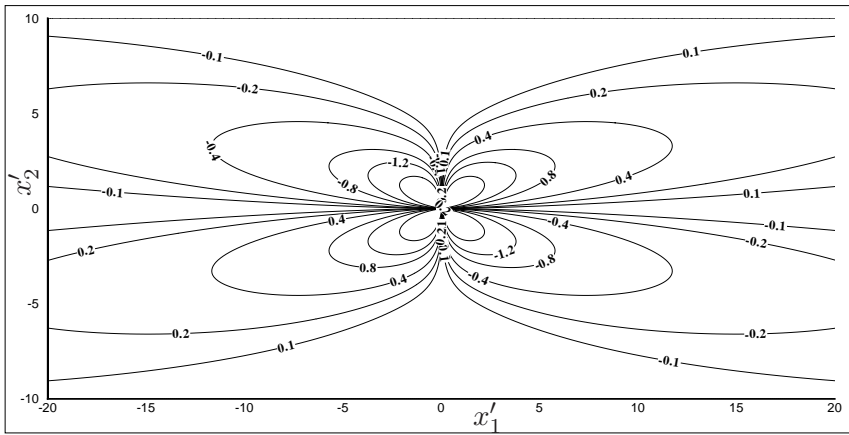


Figure 3: Isolevel contours for the velocity component $\bar{\mathbf{u}}^{(p)} \cdot \mathbf{e}_2 = \bar{\mathbf{u}}^{(n)} \cdot \mathbf{e}_1 = G_{12}(\mathbf{x}, \mathbf{x}_0) = G_{21}(\mathbf{x}, \mathbf{x}_0)$ in the plane (x'_1, x'_2) .

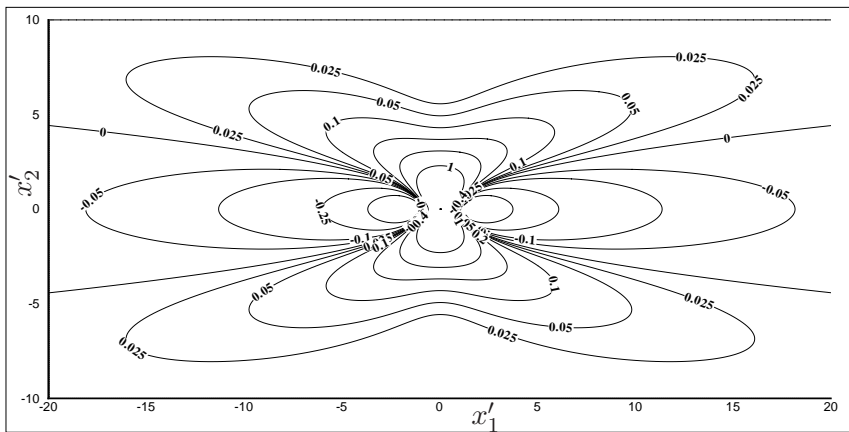


Figure 4: Isolevel contours for the velocity component $\bar{\mathbf{u}}^{(n)} \cdot \mathbf{e}_2 = G_{22}(\mathbf{x}, \mathbf{x}_0)$ in the plane (x'_1, x'_2) .

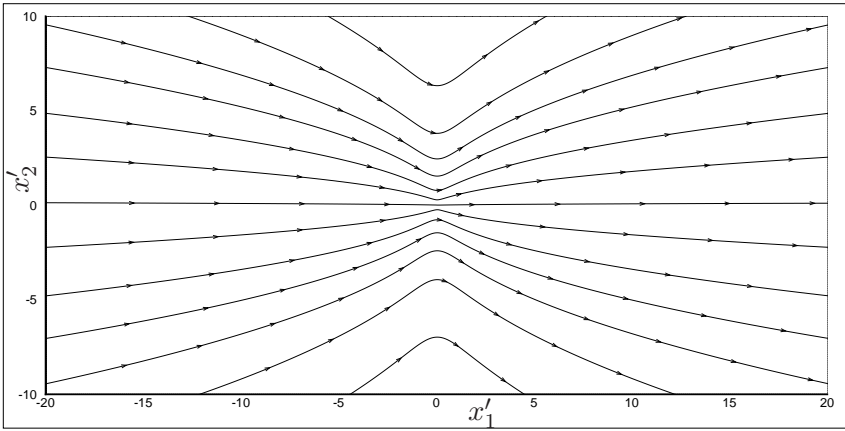


Figure 5: Streamlines for the flow $\bar{\mathbf{u}}^{(p)}$ in the plane (x'_1, x'_2) .

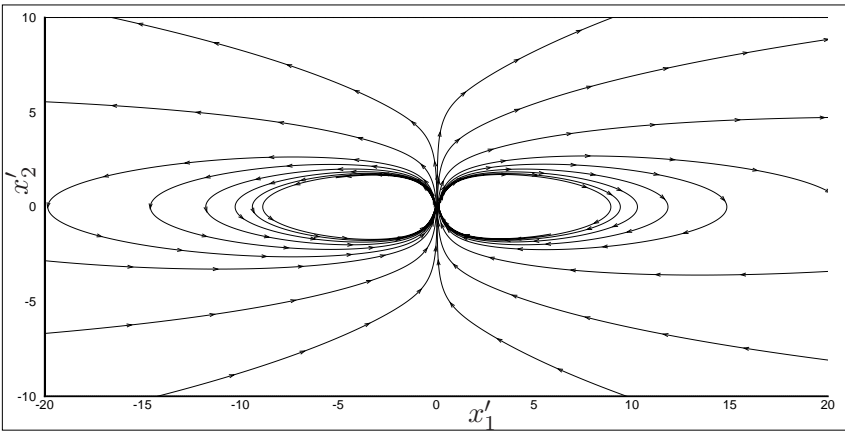


Figure 6: Streamlines for the flow $\bar{\mathbf{u}}^{(n)}$ in the plane (x'_1, x'_2) .

prescribed rigid-body motion (translation and/or rotation normal to the body). Such a challenging task requires additional efforts and is therefore postponed to a future work.

Acknowledgement: The second author (S.H. Aydin) expresses his thanks to TUBITAK (The Scientific and Technical Research Council of Turkey) for the support of the present work under programme code 2219.

References

Abramowitz, M.; Stegun, I. A. (1965): *Handbook of Mathematical Functions with Formulas, Graphs, and Mathematical Tables*. New York, 1965.

Chester, W. (1957): The effect of a magnetic field on stokes flow in a conducting fluid. *J. Fluid Mech.*, vol. 3, pp. 304–308.

Gotoh, K. (1960): Stokes flow of an electrically conducting fluid in a uniform magnetic field. *Journal of the Physical Society of Japan*, vol. 15 (4), pp. 696–705.

Hartmann, J. (1937): Theory of the laminar flow of an electrically conductive liquid in a homogeneous magnetic field. *Det Kgl. Danske Videnskabernes Selskab. Matematisk-fysiske Meddelelser*, vol. XV (6), pp. 1–28.

Jones, R. (2004): Spherical particle in Poiseuille flow between planar walls. *J. Chem. Phys.*, vol. 121, no. 1, pp. 483–500.

Moreau, R. (1990): *MagnetoHydrodynamics*. Fluid Mechanics and its Applications. Kluwer Academic Publisher, 1990.

Pozrikidis, C. (1992): *Boundary integral and singularity methods for linearized viscous flow*. Cambridge University Press.

Pozrikidis, C. (2002): *A practical guide to boundary element method with the software library BEMLIB*. London: Chapman & Hall/CRC, 2002.

Priede, J. (2013): Fundamental solutions of mhd stokes flow. *arXiv: 1309.3886v1. Physics. fluid. Dynamics*.

Sellier, A. (2008): Slow viscous motion of a solid particle in a spherical cavity. *CMES: Computer Modeling in Engineering & Sciences*, vol. 25, no. 3, pp. 165–179.

Sellier, A.; Ghalia, N. (2011): Green tensor for a general anisotropic slip condition. *CMES: Computer Modeling in Engineering & Sciences*, vol. 78, no. 1, pp. 25–50.

Sellier, A.; Pasol, L. (2006): Sedimentation of a solid particle immersed in a fluid film. *CMES: Computer Modeling in Engineering & Sciences*, vol. 16, no. 3, pp. 187–196.

Yosinobu, H.; Kabutani, T. (1959): Two-dimensional stokes flow of an electrically conducting fluid in a uniform magnetic field. *Journal of the Physical Society of Japan*, vol. 14 (10), pp. 1433–1444.